TABLE I. Clinical Findings in Affected Males Previously Reported and Our Patient

Family number: report affected males number (examined number)	1: Gilfillan et al. [2008] 3 (3)	2: Gilfillan et al. [2008] 2 (1)	3: Gilfillan et al. [2008] 3 (3)	4: Gilfillan et al. [2008], Christianson et al. [1999] 16 (4)	5: Schroer et al. [2010] 6 (6)	6: Schroer et al. [2010] 1 (1)	Our patient
Development and behavior							
Profound delay	+	+	+	+	+	+	+
Verbal language absent	+	+	+	+	+	+	+
Easily provoked laughter	+	+	+	+	3/6	−	+
CNS findings							
Epilepsy	+	+	+	+	+	+	+
Ataxia	+	+	+	+	NR	NR	+
Hyperkinetic movements	2/3	−	+	−	2/6	NR	−
Strabismus	+	+	+	+	5/6	+	+
Physical findings							
Microcephaly	+	+	+	3/4	5/6	+	+
Open mouth + drooling	2/3	+	+	NR	4/6	+	+
Swallowing difficulty	2/3	+	1/3	1/4	NR	+	−
Flexed arms	+	NR	1/3	+	3/6	−	−
Electroencephalography							
Epileptiform activity	+	+	+	+	+	+	+
Background activity	10–11 Hz	1.5–3 Hz	4–7 Hz	3–6 Hz to 11–14 Hz	NR	α rhythm	5–6 Hz
Brain MRI/autopsy							
Cerebellar atrophy	1/3	NR	NR	2/4	2/6	+	−
Mutation	p.E287_S288del c.936_941delAAAGTG	p.R500X c.1574C → T	p.V176_201del c.679 +1 delGTAA	p.H203fs c.684_685delAT	p.R500X c.1574C → T	p.Q437X c.1391C → T	p.S147fs c.441delG

+, present with all the patients; −, not present; NR, not recorded.

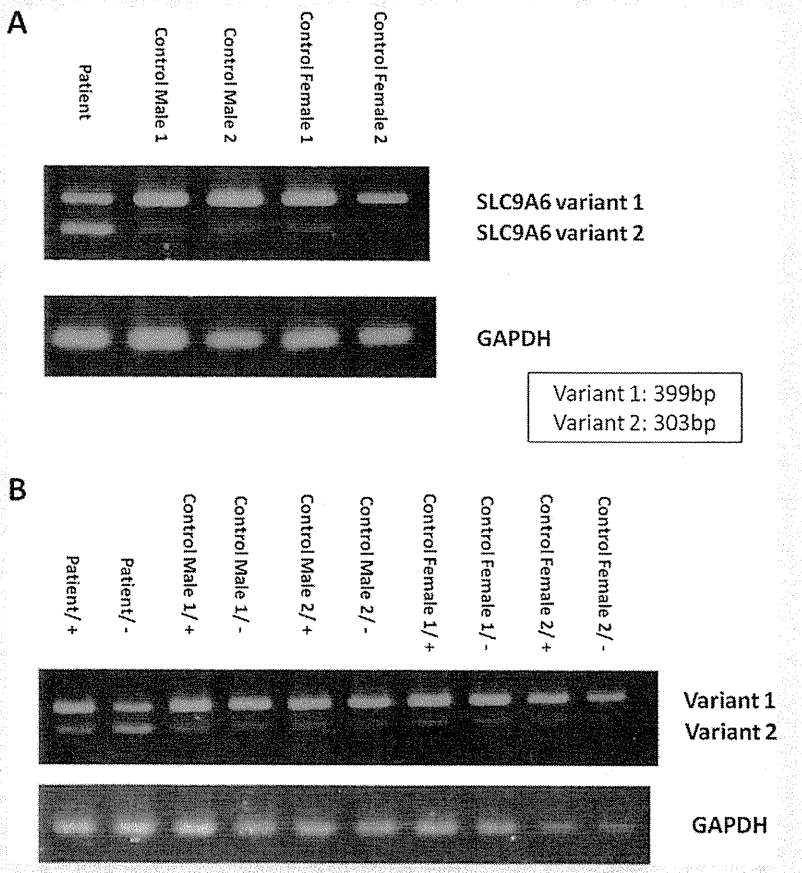

FIG. 3. RT-PCR amplification of the *SLC9A6* gene. A: *SLC9A6* variant 1 mRNA expression was decreased in the patient compared to that in four normal controls. On the other hand, variant 2 expression was increased in the patient compared to that in the controls. B: CHX treatment increases the mutant *SLC9A6* variant 1 mRNA expression, leading to similar expression levels in the patient and four normal controls samples. (+) After CHX treatment, (−) no CHX treatment.

was unchanged (Fig. 4A). The expression level of *SLC9A6* variant 2 increased in all samples after CHX treatment, however the increase was significant only in control samples (Fig. 4B).

Decreased Expression of the NHE6 Protein From Mutant *SLC9A6*

Western blotting was performed to investigate expression of the NHE6 protein in the homogenate of lymphoblastoid cell lines from the patient and his mother. As a result, protein expression of NHE6.1 was not detected in the patient (Fig. 5A,B). The same NHE6.1 was detected in HeLa cells and cells from the patient's mother as well as in the controls. NHE6.0, which was expected to be 10–20 kDa smaller than NHE6.1on SDS–PAGE [Ohgaki et al., 2008], was not detected in any sample (Fig. 5B).

DISCUSSION

In this study we investigated 22 male AS-like patients and 104 male patients with XMR, and identified only one AS-like patient with a *SLC9A6* frameshift mutation. This result further confirms *SLC9A6* is not a major cause of AS-like cases, as reported by Fichou et al. [2009]. Although the number of patients with XMR in this study was small, *SLC9A6* is likely to account for only small proportion of XMR cases.

Patients with *SLC9A6* mutations reported by Gilfillan et al., exhibit cardinal features similar to those of AS including severe developmental delay, mental retardation with absent or minimal use of words, easily provoked laughter, ataxia, epilepsy, hyperkinetic movement, nystagmus, and microcephaly.

Gilfillan et al. also identified possible features of difference between these patients and AS patients, including slow progression of symptoms, thin body, cerebellar atrophy, increased glutamate/

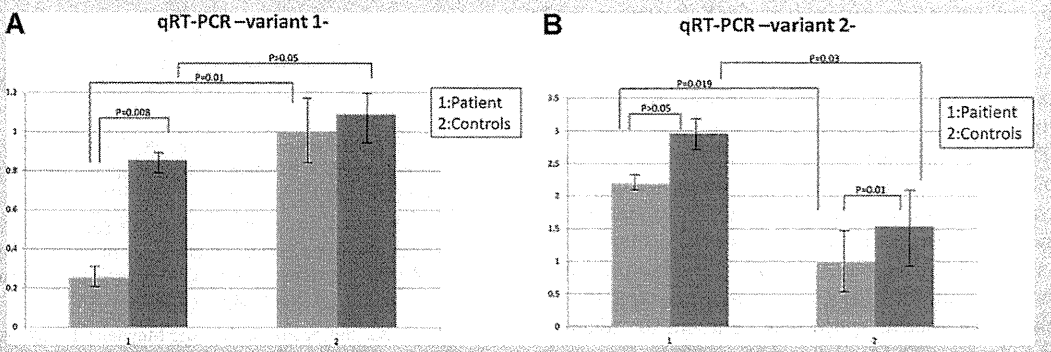

FIG. 4. Real-time quantitative PCR in samples from cell lines from the patient and four normal controls containing two males and two females. The light gray bars indicate the expression levels of *SLC9A6* before CHX treatment, while deep gray bars after CHX treatment. We performed statistical analysis using paired and unpaired Student's *t*-test. Error bars show standard deviation. A: The *SLC9A6* variant 1 was significantly downregulated in samples from the patient while it was not downregulated in samples from four normal controls. After CHX treatment, expression level of the *SLC9A6* variant 1 mRNA in the patient's sample was significantly increased. B: The *SLC9A6* variant 2 in the patient's sample was significantly increased compared to normal controls. Expression level of *SLC9A6* variant 2 increased in all samples after CHX treatment, but a significant increase was only seen in samples from controls.

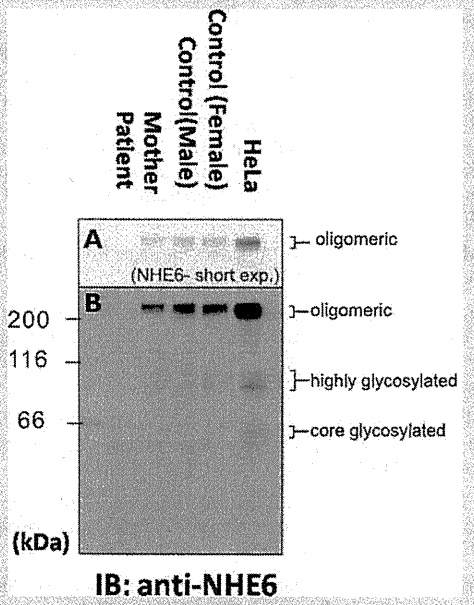

FIG. 5. Protein expression of NHE6 in cultured lymphoblastoid cells and HeLa cells. In the patient, no protein expression of NHE6 isoforms was detected with Western blotting using anti-NHE6 antibody. A: A cropped image taken using a short exposure time demonstrating the oligomeric form of NHE6. Protein size in kDa is shown by numbers on the left of the image. B: A chemiluminescence image of Western blotting taken with a longer exposure time.

glutamic acid peak on MRS, and rapid frequency of 10–14 Hz waves on EEG (Table I). Our patient lost his ability to walk although he did not demonstrate spasticity, demonstrating a slowly progressive clinical course consistent with findings in Gilfillan's report. Indeed, slow progression may be a distinctive clinical feature for patients with *SLC9A6* mutations. One of the families which Gilfillan et al. investigated was previously reported by Christianson et al. [1999], and designated as Christianson syndrome. Schroer et al. reported patients with Christianson syndrome, and they showed that the patients demonstrated an AS-like phenotype. However, while the clinical features of our patient were consistent with those of most patients previously reported by Gilfillan, there were differences including the EEG findings and lack of cerebellar atrophy. Despite this, our patient did meet the diagnostic criteria for AS [Williams et al., 2006]. Therefore, this study further demonstrated that a patient with a *SLC9A6* mutation may resemble patients with AS. Further, this striking similarity between patients with AS and those with *SLC9A6* mutations suggests a possible relationship between the gene function of *UBE3A* and *SLC9A6* in the developing brain.

Our patient's mutation created a frameshift resulting in 7 missense amino acids followed by a stop codon. This mutation was present only in *SLC9A6* transcript variant 1. *SLC9A6* mRNA has two transcript variants caused by alternative splicing in exon 2 (Fig. 1), but the role of each variant has not been clarified. The mutation detected in our patient only affects variant 1 sequence, but the phenotype of the patient was as severe as those in previously reported patients. Therefore, our finding suggests that the NHE6.1 plays an important role in brain function.

Nonsense mediated decay is involved in regulating the expression of alternatively spliced forms containing PTCs [Lareau et al., 2007; Ni et al., 2007]. Since the identified mutation was predicted to result in a PTC, we speculated that NMD could be involved in disease pathogenesis. The result of qRT-PCR showed a significant

decrease in *SLC9A6* variant 1 mRNA expression in the patient sample. This reduction was restored by CHX treatment, while *SLC9A6* variant 1 expression was unaltered by CHX treatment in normal control samples. Expression of *SLC9A6* variant 2 in the patient on the other hand, was significantly increased compared to that in control samples, however it was not influenced by CHX treatment. Therefore, the c.441delG mutation in the patient seems to have modified the alternative splicing pattern, leading to an increase in variant 2 expression. Alternatively, low variant 1 could trigger a regulatory feed back on transcription causing the apparent increase in variant 2 expression. A mutation causing premature protein truncation could alter the splicing pattern and lead to exon skipping, use of alternative splice sites, and intron retention [Hentze and Kulozik, 1999; Mendell and Dietz, 2001]. Our results indicated that the c.441delG mutation caused a PTC altered the splicing pattern, and activated NMD machinery then downregulated *SLC9A6* variant 1 expression.

As protein NHE6.1 was not detected, this indicates an absence of intact NHE6.1. NHE6.0 was also not detected. These findings conclusively indicated that the identified mutation should cause total loss-of-function. Recently, Garbern et al. identified cases with an in-frame deletion of three amino acids, who showed milder dysmorphic features and higher gross motor abilities than those in cases previously reported [Garbern et al., 2010]. Their in-frame deletion should not cause total loss-of-function but create a mildly dysfunctional protein. Therefore, severe phenotypes including severe developmental delay and progressive neurological deterioration may be caused by truncated mutations and less severe phenotypes may be caused by missense or in-frame mutations, and such mild phenotypes are likely missed in patients with mild developmental delay.

Given that the *SLC9A6* variant 2 was upregulated, we speculated that upregulated variant 2 might partially compensate for the absence of NHE6.1. However, we could not establish the upregulation of the NHE6.0 protein, rather it was not detected in the patient's lymphoblastoid cells. NHE6.0 may be unstable compared to NHE6.1. Alternately, NHE6.0 translation may be inhibited. Further investigation is required to definitively answer this question.

NHE6 is found in the membranes of early recycling endosomes and transiently in plasma membranes. Its distribution is regulated by RACK1 [Ohgaki et al., 2008]. Recycling endosomal trafficking is essential for the growth of dendritic spines during LTP in the brain [Park et al., 2006]. The function of the protein product of *UBE3A*, E3 ubiquitin ligase, is also associated with dendritic spine morphology. Mice with a maternal null mutation in *Ube3a* are also reported to have defects in LTP, and manifest motor and behavioral abnormalities [Jiang et al., 1998]. In a recent study, *Ube3a* deficient mice demonstrated dendritic spine dysmorphology [Dindot et al., 2008]. Thus, *UBE3A* and *SLC9A6* could interact in a common pathway involved in dendritic spine development, with a mutation in either leading to an AS-like phenotype.

ACKNOWLEDGMENTS

The authors thank Dr. Tadashi Ariga for critical reading of the manuscript.

REFERENCES

Aznarez I, Zielenski J, Rommens JM, Blencowe BJ, Tsui LC. 2007. Exon skipping through the creation of a putative exonic splicing silencer as a consequence of the cystic fibrosis mutation R533X. J Med Genet 44: 341–346.

Brett CL, Wei Y, Donowitz M, Rao R. 2002. Human Na(+)/H(+) exchanger isoform 6 is found in recycling endosomes of cells, not in mitochondria. Am J Cell Physiol 5:1031–1041.

Carter MS, Doskow J, Morris P, Li S, Nhim RP, Sandstedt S, Wilkinson MF. 1995. A regulatory mechanism that detects premature nonsense codons in T-cell receptor transcripts in vivo is reversed by protein synthesis inhibitors in vitro. J Biol Chem 270:28995–29003.

Christianson AL, Stevenson RE, van der Meyden CH, Pelser J, Theron FW, van Rensburg PL, Chandler M, Schwartz CE. 1999. X linked severe mental retardation, craniofacial dysmorphology, epilepsy, ophthalmoplegia, and cerebellar atrophy in a large South African kindred in localized to Xq24–q27. J Med Genet 36:759–766.

Dindot SV, Antalffy BA, Bhattacharjee MB, Beaudet AL. 2008. The Angelman syndrome ubiquitin ligase localizes to the synapse and nucleus, and maternal deficiency results in abnormal dendritic spine morphology. Hum Mol Genet 17:111–118.

Fichou Y, Bahi-Buisson N, Nectoux J, Chelly J, Heron D, Cuisset L, Bienvenu T. 2009. Mutation in the *SLC9A6* gene is not a frequent cause of sporadic Angelman-like syndrome. Eur J Hum Genet 17:1378–1380.

Garbern JY, Neumann M, Trojanowski JQ, Lee VM, Feldman G, Norris JW, Friez MJ, Schwartz CE, Stevenson R, Sima AA. 2010. A mutation affecting the sodium/proton exchanger, *SLC9A6*, causes mental retardation with tau deposition. Brain 133:1391–1402.

Gilfillan GD, Selmer KK, Roxrud I, Smith R, Kyllerman M, Eiklid K, Kroken M, Mattingsdal M, Egeland T, Stenmark H, Sjoholm H, Server A, Samuelsson L, Christianson A, Tarpey P, Whibley A, Stratton MR, Futreal A, Teague J, Edkins S, Gecz J, Turner G, Raymond FL, Schwartz C, Stevenson RE, Undlien DE, Stromme P. 2008. *SLC9A6* mutations cause X-linked mental retardation, microcephaly, epilepsy, and ataxia, a phenotype mimicking Angelman Syndrome. Am J Hum Genet 82: 1003–1010.

Hentze MW, Kulozik AE. 1999. A perfect message: RNA surveillance and nonsense-mediated decay. Cell 96:307–310.

Jiang YH, Armstrong D, Albrecht U, Atkins CM, Noebels JI, Eichele G, Sweatt JD, Beaudet AL. 1998. Mutation of the Angelman ubiquitin ligase in mice causes increased cytoplasmic p53 and deficits of contextual learning and long-term potentiation. Neuron 21:799–811.

Lareau LF, Inada M, Green RE, Wengrod JC, Brenner SE. 2007. Unproductive splicing of SR genes associated with highly conserved and ultraconserved DNA elements. Nature 446:926–929.

Mendell JT, Dietz HC. 2001. When the message goes awry: Disease-producing mutations that influence mRNA content and performance. Cell 107:411–414.

Nakamura N, Tanaka S, Teko Y, Mitsui K, Kanazawa H. 2005. Four Na^+/H^+ exchanger isoforms are distributed to Golgi and post-Golgi compartments and are involved in organelle pH regulation. J Biol Chem 280:1561–1572.

Ni JZ, Grate L, Donohue JP, Preston C, Nobida N, O'Brien G, Shiue L, Clark TA, Blume JE, Ares M, Jr. 2007. Ultraconserved elements are associated with homeostatic control of splicing regulators by alternative splicing and nonsense-mediated decay. Genes Dev 21:708–718.

Ohgaki R, Fukura N, Matsushita M, Mitsui K, Kanazawa H. 2008. Cell surface levels of organellar Na^+/H^+ exchanger isoform 6 are regulated by interaction with RACK1. J Biol Chem 283:4417–4429.

Park M, Salgado JM, Ostroff L, Helton TD, Robinson CG, Harris KM, Ehlers MD. 2006. Plasticity-induced growth of dendritic spines by exocytic trafficking from recycling endosomes. Neuron 52:817–830.

Roxrud I, Raiborga C, Gilfillan GD, Strømmed P, Stenmark H. 2009. Dual degradation mechanisms ensure disposal of NHE6 mutant protein associated with neurological disease. Exp Cell Res 135:3014–3027.

Saitoh S, Wada T, Okajima M, Takano K, Sudo A, Niikawa N. 2005. Uniparental disomy and imprinting defects in Japanese patients with Angelman syndrome. Brain Dev 27:389–391.

Schroer RJ, Holden KR, Tarpey PS, Matheus MG, Griesemer DA, Friez MJ, Fan JZ, Simensen RJ, Stromme P, Stevenson RE, Stratton MR, Schwartz CE. 2010. Natural history of Christianson syndrome. Am J Med Genet Part A 152A:2775–2783.

Takano K, Nakagawa E, Inoue K, Kamada F, Kure S, Goto Y, Japanese Mental Retardation Consortium. 2008. A loss-of-function mutation in the FTSJ1 gene causes nonsyndromic X-linked mental retardation in a Japanese family. Am J Med Genet Part B 147B:479–484.

Williams CA, Beaudet AL, Clayton-Smith J, Knoll JH, Kyllerman M, Laan LA, Magenis RE, Moncla A, Schinzel AA, Summers JA, Wagstaff J. 2006. Angelman Syndrome 2005: Updated consensus for diagnostic criteria. Am J Med Genet Part A 140A:413–418.

The Journal of Laryngology & Otology, 1 of 4.

doi:10.1017/S0022215111002453

CLINICAL RECORD

Successful cochlear implantation in a patient with mitochondrial hearing loss and m.625G>A transition

A SUDO[1], N TAKEICHI[2], K HOSOKI[3], S SAITOH[3]

[1]*Department of Pediatrics, Sapporo City General Hospital, and the Departments of* [2]*Otolaryngology and* [3]*Pediatrics, Hokkaido University Graduate School of Medicine, Sapporo, Japan*

Abstract

Objective: We present a patient with mitochondrial hearing loss and a novel mitochondrial DNA transition, who underwent successful cochlear implantation.

Case report: An 11-year-old girl showed epilepsy and progressive hearing loss. Despite the use of hearing aids, she gradually lost her remaining hearing ability. Laboratory data revealed elevated lactate levels, indicating mitochondrial dysfunction. Magnetic resonance imaging showed diffuse, mild brain atrophy. Cochlear implantation was performed, and the patient's hearing ability was markedly improved. Whole mitochondrial DNA genome analysis revealed a novel heteroplasmic mitochondrial 625G>A transition in the transfer RNA gene for phenylalanine. This transition was not detected in blood DNA from the patient's mother and healthy controls. Mitochondrial respiratory chain activities in muscle were predominantly decreased in complex III.

Conclusion: This case indicates that cochlear implantation can be a valuable therapeutic option for patients with mitochondrial syndromic hearing loss.

Key words: Sensorineural Hearing Loss; Cochlear Implantation; Mitochondrial DNA

Introduction

There have recently been many reported cases of sensorineural hearing loss of mitochondrial origin. In such patients, the effectiveness of cochlear implantation has been recognised in those with the m.1555A>G and m.3243A>G mutations.[1] However, the efficacy of such treatment for patients with other mitochondrial DNA mutations has not yet been defined.

Here, we present a patient with syndromic hearing loss, probably caused by a novel mitochondrial DNA mutation (m.625G>A), who gained excellent benefit from cochlear implantation.

Case report

The patient, an 11-year-old girl, was the first child of healthy and nonconsanguineous Japanese parents. There was no family history of hearing loss or epilepsy, and the patient had had no perinatal problems. Her motor and cognitive development was normal, but she displayed an abnormally short stature for her age.

The patient's hearing difficulty had first been noticed by her mother at the age of six years. Two years later, the patient had been examined by an otolaryngologist for the first time, and bilateral hearing aids had been prescribed. However, her hearing ability continued to deteriorate. There had been no previous exposure to aminoglycoside antibiotics. In addition to hearing loss, at the age of eight years the patient had begun to suffer generalised tonic seizures, uncontrolled by valproic acid. At the age of 10 years, she had been referred to our institution, as her family had moved to the locality near our hospital.

On physical examination, the patient had a height of 119.0 cm (−3.0 standard deviations (SD)), a weight of 21.9 kg (−1.7 SD) and a head circumference of 53.6 cm (+0.9 SD). Cranial nerve and cerebellar functions were normal. Hypertrichosis was observed. Although her muscle force did not decrease, she was unable to exercise for extended periods of time. Deep tendon reflexes were normal, without spasticity. She was unable to communicate verbally, although her intelligence appeared normal as she could communicate in writing and could solve age-appropriate arithmetic problems. Otitis media was not found.

Laboratory data revealed mildly elevated blood lactate levels (24.0 mg/dl (normal range, <17 mg/dl), with a pyruvate level of 1.0 mg/dl (normal range, <0.9 mg/dl)), and noticeably elevated cerebrospinal fluid lactate levels (55.8 mg/dl, with a pyruvate level of 2.0 mg/dl).

Electroencephalography revealed no distinct epileptic discharge during waking and sleeping states.

Computed tomography showed no internal ear malformations. Magnetic resonance imaging (MRI) revealed mild brain atrophy without focal lesions (Figure 1a).

Abstract presented at the 9th Conference of the Japanese Society of Mitochondrial Research and Medicine, 18 December 2009, Tokyo, Japan
Accepted for publication 31 March 2011

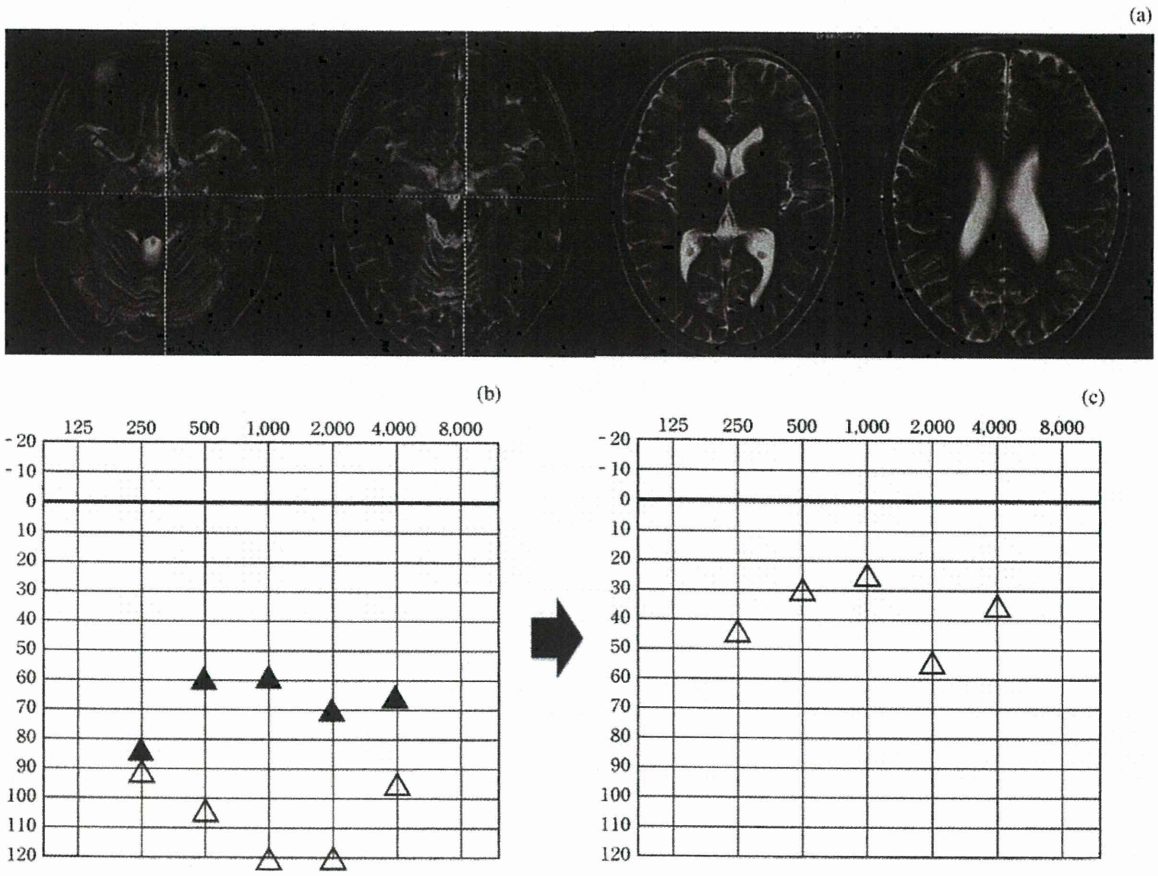

FIG. 1

(a) Axial magnetic resonance imaging brain scans, showing mild brain atrophy without focal lesions. (b) Left ear audiogram taken at 11 years, before cochlear implantation, following progression of hearing loss (hearing aids were no longer useful). (c) Left ear audiogram taken one month after implantation, showing significant improvement, with hearing thresholds of almost 25 – 45 dB. Δ = sound source 1 m away, without hearing aids; ▲ = with hearing aids in both ears

Formal pure tone audiography revealed hearing thresholds of between 90 and 120 dB at 250 through to 4 kHz. The patient's hearing aids only minimally improved her hearing thresholds (Figure 1b).

Auditory evoked potential testing showed a barely detectable auditory reaction at maximum intensity stimulation of 105 dB.

Therefore, the patient was considered to be a candidate for cochlear implantation.

Informed consent for participation in academic research was obtained from the patient and her parents.

During cochlear implantation, temporalis muscle and skin specimens were obtained.

Genomic DNA was extracted from blood, skin and muscle specimens. Sequencing of the whole mitochondrial genome was performed using the mitoSEQ resequencing system (Applied Biosystems, Foster City, California, USA). Polymerase chain reaction amplification was conducted, using forward mismatch primer (nucleotides 601–624, 5′-GCAATACACTGAAAATGTTTAGC-3′; where G = guanine, C = cytosine, A = adenine and T = thymine) and reverse primer (nucleotides 768–786, 5′-CGTTTTGAG CTGCATTGCT-3′). This enabled the m.625G>A sequence to be specifically recognised, and cut using the restriction enzyme BstOI (Promega, Madison, WI, USA). The proportion of heteroplasmy was approximately measured by using a mixture-template standard curve of wild type and mutant clones.

The activities of the mitochondrial respiratory chain complexes I, II, III and IV were assayed, using methods previously described.[2] We used the diagnostic criteria for respiratory chain disorders previously published by Bernier *et al.*[3]

Cochlear implantation and clinical course

The patient underwent left-sided cochlear implantation (using a CI24RCS device; cochlear LTD, Lane Cove, Australia) at the age of 11 years.

One month after implantation, she was able to use the telephone, clearly indicating improvement in her hearing function. Audiological data indicated a good response (Figure 1c). Her speech perception score increased to almost 100 per cent, from 0 per cent before surgery.

Twenty months after surgery, the patient and her parents were satisfied with her improved communication, and she continued to attend regular school classes. Her epileptic seizures were well controlled by carbamazepine and clonazepam. Her neurological signs and symptoms remained nonprogressive, possibly due to vitamin B1 supplementation.

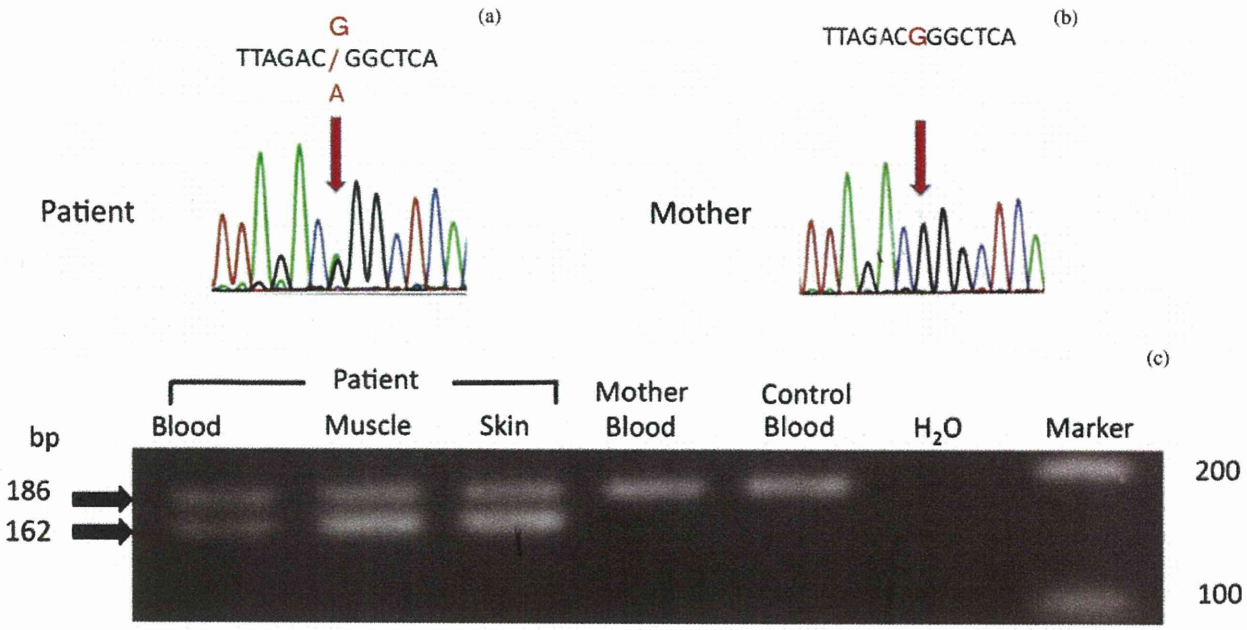

FIG. 2

Detection of the heteroplasmic m.625G>A transition. Diagrams represent screening of the patient's peripheral blood (a) and her mother's peripheral blood (b) for whole mitochondrial DNA genomes, and show the heteroplasmic m.625G>A transition in the patient's blood but not the mother's blood. (c) Electrophoretic strip showing that, in the presence of the m.625G>A mutation, the 186 base pair (bp) fragment was cleaved into 162 and 24 bp fragments (the latter not shown) by (BstOI is manufactured by Promega, Madison, WI, USA). This mutation was present in a heteroplasmic state in the patient's blood, muscle and skin, but was not detected in the mother's blood. Wild-type clones contained only the m.625G sequence.

Histological analysis

Unfortunately, many artifactual opaque fibers were observed in the temporalis muscle biopsy. Nevertheless, a few cytochrome c oxidase (COX) negative fibres were identified, although there were no ragged red fibres or strongly succinate dehydrogenase (SDH) reactive blood vessels (data not shown).

Genetic analysis

Whole mitochondrial DNA genome analysis, using peripheral blood DNA, detected two heteroplasmic base transitions: m.625G>A (Figure 2a) and m.5231G>A (data not shown).

The m.625G>A transition was present in a heteroplasmic state in the patient's blood, muscle and skin, but was not detected in her mother's blood (Figures 2b). The proportion of m.625G>A in muscle and skin was higher than that in blood (the approximate mutation load was 80 per cent in muscle and skin, and 70 per cent in blood) (Figure 2c). This transition was not present in 50 healthy controls.

The heteroplasmic m.5231G>A transition was present in both the patient's and her mother's blood.

Biochemical analysis

Respiratory chain enzyme assay showed that complex III activity was markedly decreased (30 per cent relative to citrate synthase, 17 per cent relative to complex II) while complex IV activity was slightly decreased (55 per cent relative to citrate synthase, 31 per cent relative to complex II).

Discussion

Mitochondrial sensorineural hearing loss is divided into the nonsyndromic type associated with m.1555A>G and the syndromic type associated with m.3243A>G. The complex of mitochondrial encephalopathy, lactic acidosis and stroke-like episodes (known as MELAS) is representative of the latter.[1]

We considered our case to be the syndromic type, because the patient had short stature and suffered from hypertrichosis and epilepsy. Moreover, she showed high lactate levels in her blood and cerebrospinal fluid, and mild brain atrophy on MRI.

In the syndromic type of mitochondrial hearing loss, the retrocochlear auditory pathways require investigation, specifically to establish whether the auditory peripheral nerve and central nervous system (CNS) are intact or not. However, successful cochlear implantation has been reported in patients with the mitochondrial encephalopathy, lactic acidosis and stroke-like episode complex.[4–6] Sue *et al.* have reported successful cochlear implantation in such a patient, who had profound, bilateral hearing loss.[6]

Our case, too, underwent successful cochlear implantation, despite possible CNS disorders. In patients with many types of mitochondrial, profound, sensorineural hearing loss, we speculate that cochlear implantation may represent a promising treatment, because hearing loss associated with mitochondrial disorders is more likely to be caused by cochlear dysfunction than retrocochlear abnormalities.[1,6,7] Results from a guinea pig cochlear model also suggest that chronic mitochondrial dysfunction may most predominantly affect the stria vascularis and supporting cells.[8] Therefore, we believe that cochlear implantation should be considered in patients with progressive sensorineural hearing loss associated with a mitochondrial disease, regardless of whether their hearing loss is syndromic or nonsyndromic.

Of course, this treatment option should be reviewed for the potential complications; it may develop contraindications on the MRI scan (unless the magnet in the receiver-stimulator has been moved), or adverse events such as post-implant meningitis due to bacterial cellulitis.[9]

In our patient, whole mitochondrial DNA genome analysis detected two different heteroplasmic, one-base substitutions: m.625G>A and m.5231G>A.

Although heteroplasmic single nucleotide polymorphisms are rare, the m.5231G>A transition is unlikely to be pathogenic, because it has been listed as a single nucleotide polymorphism in the Mitomap database,[10] and because it was carried by our patient's healthy mother.

On the other hand, the m.625G>A transition (which involves the transfer RNA gene for phenylalanine) has not previously been reported in association with disease. This transition lies in close vicinity to the site of the m.622G>A mutation, which has been reported to be present in mild mitochondrial disease with hearing impairment.[11] Moreover, other mutations in the same transfer RNA gene for phenylalanine (e.g. m.582T>C, m.583G>A, m.606A>G, m.608A>G, m.611G>A, m.618T>C, m.636A>G and m.642T>C) have been recognised and listed in Mitomap, with deafness frequently mentioned as a clinical symptom.[12–14] In our patient, respiratory enzyme studies revealed a significant defect in complex III and a possible slight defect in complex IV, relative to citrate synthase and complex II. These results resembled those for other mutations of the same mitochondrial transfer RNA gene for phenylalanine, such as m.622G>A and m.618T>C.[11,15] Moreover, m.625G>A was not identified in our patient's mother's peripheral blood DNA, implying a *de novo* origin of the mutation, although this is not conclusive because only blood DNA was available from the mother. Such sporadic mutations have been reported in other patients with the same mitochondrial transfer RNA phenylalanine gene mutation.[12,16]

- **This report describes the case of a girl with mitochondrial sensorineural hearing loss**
- **Cochlear implantation was effective, and improved the patient's quality of life**
- **The mitochondrial DNA 625G>A mutation may be pathogenic for syndromic hearing loss**

Accordingly, we conclude that the m.625G>A transition may cause mitochondrial respiratory dysfunction and syndromic hearing loss. Another standard muscle biopsy and cybrid study would clarify the pathogenicity of the m.625G>A transition.

Conclusion

We report a sporadic case of progressive sensorineural hearing loss and epilepsy due to a mitochondrial disorder, successfully treated with cochlear implantation. The novel, heteroplasmic m.625G>A transition in the mitochondrial transfer RNA gene for phenylalanine may have been the pathogenic mutation in this case.

Cochlear implantation should be considered for patients with progressive, profound, bilateral, sensorineural hearing loss due to mitochondrial disease other than that due to the m.3243A>G mutation of the transfer RNA (tRNA(leu)) gene, or the m.1555A>G mutation of the 12s rivosomal RNA.

Acknowledgements

We are grateful to Dr Kei Murayama and Dr Akira Ohtake for their enzyme study and helpful comments. We also thank Dr Ichizo Nishino for muscle pathology analysis. This work was partially supported by a grant from the Ministry of Education, Science and Culture of Japan.

References

1 Sinnathuray AR, Raut V, Awa A, Magee A, Toner JG. A review of cochlear implantation in mitochondrial sensorineural hearing loss. *Otol Neurotol* 2003;**24**:418–26
2 Rahman S, Blok RB, Dahl H-HM, Danks DM, Kirby DM, Chow CW *et al.* Leigh syndrome: clinical features and biochemical and DNA abnormalities. *Ann Neurol* 1996;**39**:345–51
3 Bernier FP, Boneh A, Dennett X, Chow CW, Cleary MA, Thorburn DR. Diagnostic criteria for respiratory chain disorders in adults and children. *Neurology* 2002;**59**:1406–11
4 Rosenthal EL, Kileny PR, Boerst A, Telian SA. Successful cochlear implantation in a patient with MELAS syndrome. *Am J Otol* 1999;**20**:187–91
5 Karkos PD, Anari S, Johnson IJ. Cochlear implantation in patients with MELAS syndrome. *Eur Arch Otorhinolaryngol* 2005;**262**:322–4
6 Sue CM, Lipsett LJ, Crimmins DS, Tsang CS, Boyages SC, Presgrave CM. Cochlear origin of hearing loss in MELAS syndrome. *Ann Neurol* 1998;**43**:350–9
7 Yamasoba T, Tsukuda K, Oka Y, Kobayashi T, Kaga K. Cochlear histopathology associated with mitochondrial transfer $RNA^{Leu(UUR)}$ gene mutation. *Neurology* 1999;**52**:1705–7
8 Yamasoba T, Goto Y-I, Komaki H, Mimaki M, Sudo A, Suzuki M. Cochlear damage due to germanium-induced mitochondrial dysfunction in guinea pigs. *Neurosci Lett* 2006;**395**:18–22
9 Papsin BC, Gordon KA. Cochlear implants for children with severe-to-profound hearing loss. *N Engl J Med* 2007;**357**:2380–7
10 mtDNA Coding Region Sequence Polymorphism. In: http://www.mitomap.org/bin/view/MITOMAP/Polymorphisms Coding [6 August 2011]
11 Deschauer M, Swalwell H, Strauss M, Zierz S, Taylor RW. Novel mitochondrial transfer RNA (Phe) gene mutation associated with late-onset neuromuscular disease. *Arch Neurol* 2006;**63**:902–5
12 Mancuso M, Filosto M, Mootha VK, Rocchi A, Pistolesi S, Murri L. A novel mitochondrial tRNAPhe mutation causes MERRF syndrome. *Neurology* 2004;**62**:2119–21
13 Konings A, Van Camp G, Goethals A, Eyken EV, Vandevelde A, Azza JB *et al.* Mutation analysis of mitochondrial DNA 12SrRNA and tRNASer(UCN) genes in non-syndromic hearing loss patients. *Mitochondrion* 2008;**8**:377–82
14 Valente L, Piga D, Lamantea E, Carrara F, Uziel G, Cudia P *et al.* Identification of novel mutations in five patients with mitochondrial encephalomyopathy. *Biochim Biophys Acta* 2009;**1787**:491–501
15 Kleinle S, Schneider V, Moosmann P, Brandner S, Krähenbühl S, Liechti-Gallati S. A novel mitochondrial $tRNA^{Phe}$ mutation inhibiting anticodon stem formation associated with a muscle disease. *Biochem Biophys Res Commun* 1998;**247**:112–15
16 Darin N, Kollberg G, Moslemi AR, Tulinius M, Holme E, Grönlund MA *et al.* Mitochondrial myopathy with exercise intolerance and retinal dystrophy in a sporadic patient with a G583A mutation in the mt tRNA(phe)gene. *Neuromuscul Disord* 2006;**16**:504–6

Address for correspondence:
Dr A Sudo,
Department of Pediatrics,
Sapporo City General Hospital,
Kita 11,
Nishi 13, Chuo-ku,
Sapporo 060-8604, Japan

Fax: +81 11 726 7912
E-mail: akira.sudo@doc.city.sapporo.jp

Dr A Sudo takes responsibility for the integrity of the content of the paper
Competing interests: None declared

Pediatrics International (2012) ••, ••–••

doi: 10.1111/j.1442-200X.2011.03550.x

Patient Report

Hand-foot-genital syndrome with a 7p15 deletion: Clinically recognizable syndrome

Kana Hosoki,[1] Tohru Ohta,[2] Keinosuke Fujita,[3] Satsuki Nishigaki,[3] Masashi Shiomi,[4] Norio Niikawa[2] and Shinji Saitoh[1,5]

[1]*Department of Pediatrics, Hokkaido University Graduate School of Medicine, Sapporo,* [2]*Research Institute of Personalized Health Sciences, Health Science University of Hokkaido, Tobetsu, Departments of* [3]*Pediatrics and* [4]*Pediatric Emergency Medicine, Osaka City General Hospital, Osaka and* [5]*Department of Pediatrics and Neonatology, Nagoya City University School of Medical Sciences, Nagoya, Japan*

Key words developmental delay, hand-foot-genital syndrome, *HOXA* cluster, *HOXA13*, 7p15 deletion.

Hand-foot-genital syndrome (HFGS; MIM 140000) is a congenital limb malformation syndrome involving small hands and feet with unusually short great toes and abnormal thumbs.[1] HFGS is caused by mutations in *HOXA13* located on 7p15.2, a *HOXA* family member that correlates to construct patterning of the vertebrate.[2] Patients with a deletion encompassing *HOXA13* also have typical features of HFGS.[3]

Many deletions involving 7p15 have been reported. All deletions involving *HOXA13* include HFGS features.[3–6] Nevertheless, because larger deletions often show severe clinical features, HFGS phenotypes may not be recognized in such large-deletion cases. In contrast, patients with smaller deletions involving 7p15 appear to have mild developmental delay and characteristic facies in association with HFGS.[5,6]

Here we report on a patient with a 6.9 Mb deletion at 7p15. Compared to previous studies, we propose that a small deletion of 7p15 causes a clinically recognizable syndrome.

Case report

Patient

The boy was born at 39 weeks of gestation as the fourth child of healthy parents. Other family members were also healthy. His birthweight, length, and head circumference were 2560 g (–1.2 SD), 48.0 cm (–0.5 SD), and 32.5 cm (–0.2 SD), respectively. In the neonatal period he developed feeding difficulty. He showed mild developmental delay, and acquired head control at age 3 months, rolling over at 7 months, unassisted walk at 14 months, and meaningful words at 15 months.

At age 10 years he was suspected of having Prader–Willi syndrome (PWS) for his small hands and feet, short stature, developmental delay, feeding difficulty during infancy and mild obesity, which developed after childhood. Examination at 13 years showed a height of 138 cm (–2.5 SD), and a weight of 44 kg (–0.5 SD). He exhibited mildly dysmorphic facies including bifrontal narrowing and low-set posterior rotated dysplastic ears (Fig. 1a,d). He did not have ophthalmological or audiological complications. He had small hands and feet with clinodactyly of the bilateral fifth finger, and short, curved and broad great toes (Fig. 1b,e,g). X-ray demonstrated small pointed distal phalanges and hypoplastic middle phalange of the fifth digits (Fig. 1c), and hypoplasia of the middle and distal phalanges (Fig. 1f). Bone age at 10 years 4 months was delayed and estimated to be 6 years 6 months. Genital anomaly was not present. He did not have intellectual or behavioral problems and attended regular primary school although a formal IQ test has not been done.

Prader–Willi syndrome and maternal uniparental disomy 14 (upd(14)mat) syndrome was excluded on genetic tests (data not shown),[7] and G-band chromosomal analysis showed a normal karyotype of 46,XY. Microarray analysis was then performed, as described in the following section.

DNA methylation analysis

Genomic DNA was isolated from peripheral blood leukocytes of the patient and his parents. DNA-methylation-specific polymerase chain reaction for *SNRPN* at 15q11.2 and *MEG3* at 14q32.2 was performed as described previously to rule out PWS and upd(14)mat syndromes.[7]

Microarray analysis

We performed a chromosomal microarray analysis using Genome-Wide Human SNP Nsp/Sty Array Kit 5.0 (Affymetrix, Santa Clara, CA, USA) for genomic DNA isolated from peripheral blood leukocytes of the patient and his parents. Microarray analysis of the patient detected a 6.9 Mb deletion at 7p15.3-p15.1 [arr7p15.3p15.1(22 460 185–29 360 960)x1] (Fig. 2). This deletion was not identified in his parents, indicating the de novo origin of the deletion. Single nucleotide polymorphism (SNP) genotyping in the deleted region showed that the deletion was of

Correspondence: Shinji Saitoh, MD PhD, Department of Pediatrics and Neonatology, Nagoya City University School of Medical Sciences, Kawasumi 1, Mizuho-cho, Mizuho-ku, Nagoya 467-8601, Japan. Email: ss11@med.nagoya-cu.ac.jp

Received 28 June 2011; revised 24 October 2011; accepted 9 November 2011.

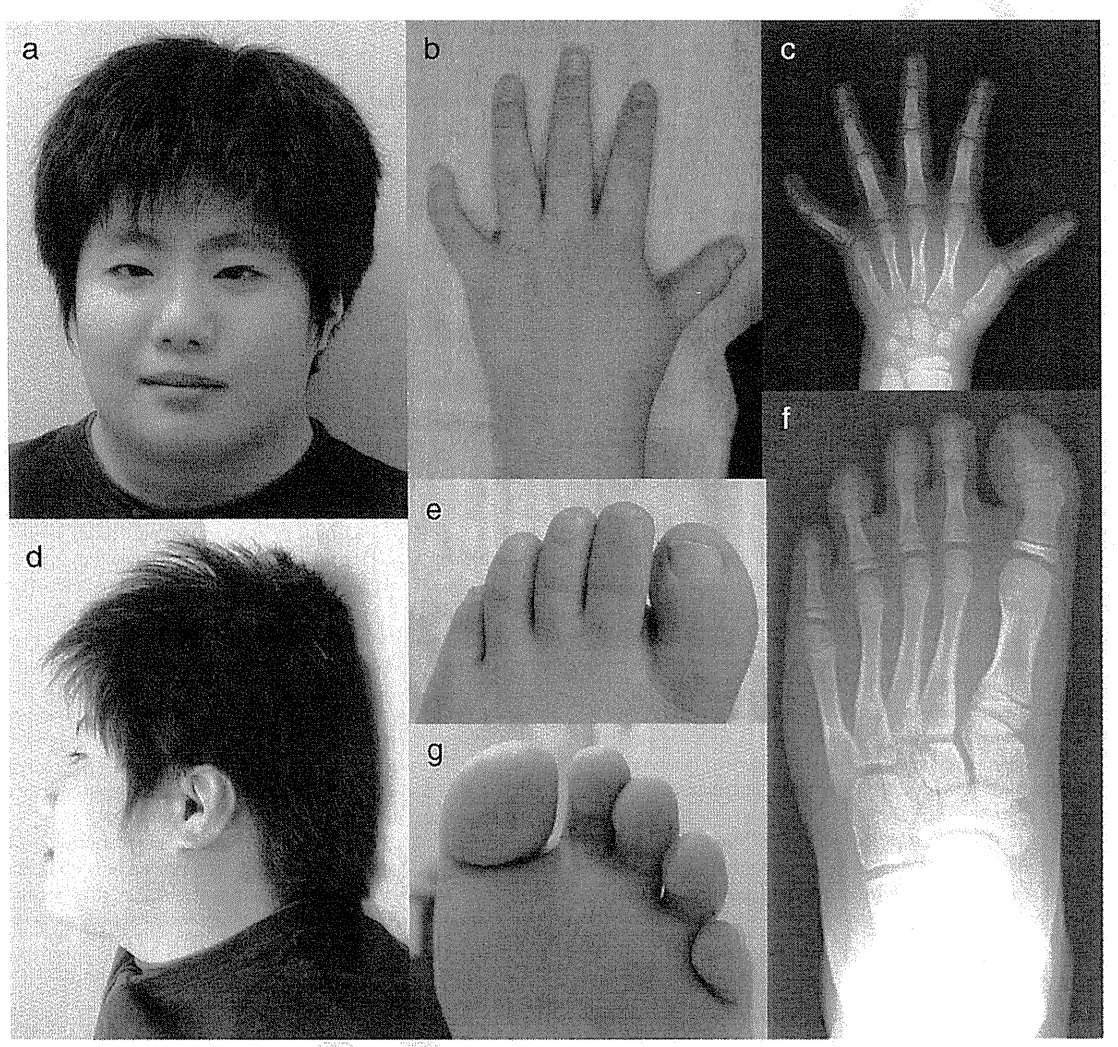

Fig. 1 Facial expression and limb abnormalities in the present patient. (a) Mildly dysmorphic facies with bifrontal narrowing. (d) Lateral view demonstrating low-set posterior rotated dysplastic ears. (b) Left hand showing short digits and clinodactyly of the fifth finger. (c) X-ray showing small pointed distal phalanges and hypoplasia of the middle phalange of the fifth digit. (e,g) Left foot showing a short, curved and broad great toe. (f) X-ray showing hypoplasia of the middle and distal phalanges.

paternal origin (data not shown). The deletion contained the *HOXA* cluster including *HOXA13* as well as 56 other genes (Fig. 2).

Discussion

Hand-foot-genital syndrome caused by a deletion encompassing *HOXA13* shows additional features, such as mildly dysmorphic facies, developmental delay, feeding difficulty in the neonatal period, and borderline mentality or intellectual disability.[3,5,6] Four patients with a small deletion involving *HOXA13* located at 7p15 have been reported.[3,5,6] The present patient, with manifestations similar to those of the four previous cases, had a deletion containing *HOXA13*. This let us make further delineation of HFGS, that is, 'deletion-positive' (deletion+) HFGS (Table 1). Although the ear, nose and eye of the five patients with deletion+ HFGS were mildly dysmorphic, their facial characteristics remained inconclusive. Developmental delay, albeit mild, was present in all five patients, and intelligence varied from normal to mildly disabled. It is noteworthy that three of the five patients had neonatal feeding difficulty. Deletion+ HFGS may involve developmental

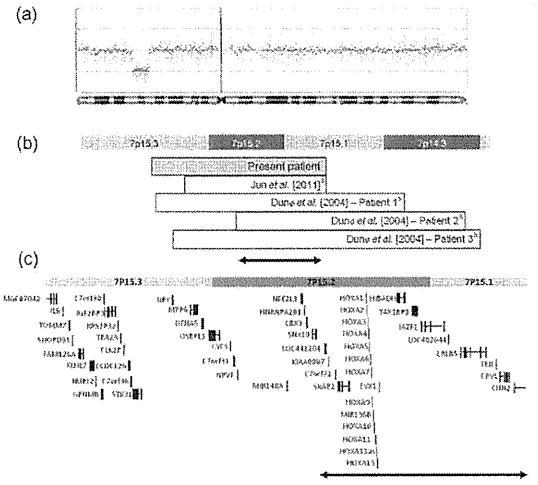

Fig. 2 Microarray results of the patient. (a) 6.9 Mb interstitial deletion at 7p15.3-p15.1 [arr7p15.3p15.1(22 460 185–29 360 960)x1]. (b) Overlapping deletions of five patients.[5,6] Shortest region of overlap (SRO; arrow) is approximately 2 Mb. (c) Schematic of included genes in the deletion region. Genome coordinates are according to the 36.1 build (March 2006) of the human reference genome at the UCSC database (http://genome.ucsc.edu/). The SRO (arrow) is defined from the proximal border of the deletion of Dunø *et al.*'s patient 2 to the distal border of that of the present patient (chr7:26 374 754–29 360 960), containing nine genes plus *HOXA* cluster.[5] In addition, the Dunø *et al.* reported positions were arranged from the 34 build (July 2003) to 36.1 build.[5]

delay, feeding difficulty in the neonatal or infantile period and short stature in addition to small hands/feet and genital anomaly. Therefore, it is possible that the patients could be suspected to have PWS. This pattern of abnormalities might cause attending physicians to suspect PWS, as was the case for the present patient. Nevertheless, limb abnormalities of HFGS are distinct from those of PWS. Bone abnormalities frequently found in HFGS are not present in PWS. Therefore, detailed clinical investigation including X-ray examination of hands and feet may be of help to differentiate HFGS from PWS.

The 2.0 Mb shortest region of overlap (SRO) among the five patients with deletion+ HFGS is defined from the proximal border of the deletion of Dunø *et al.*'s patient 2 to the distal border of that of the present patient, and should define its critical region (Fig. 2).[5] The exact breakpoints of Jun *et al.*'s patient were not certain because the reference sequence was not provided, but the distal breakpoint should be similar to that of the present patient because it was located between *STK31* and *CHN2*.[6] Because the distal breakpoint of the present patient is located within 7p15.1, several genes located more distally are excluded from candidacy for deletion+ HFGS. The SRO among the five patients contains nine genes other than the *HOXA* cluster (Fig. 2). Among the nine genes, only *JAZF1* (*TIP27*) was designated as a morbid gene, according to the OMIM database (http://www.ncbi.nlm.nih.gov/omim/). *JAZF1* was initially identified as a 7p15-derived participant in the fusion gene resulting from t(7;17)(p15;q21) translocation in endometrial stromal sarcoma cells.[8] Genome-wide association study demonstrated that an SNP in *JAZF1* is associated with type 2 diabetes, but there have been

Table 1 Clinical features on five patients with 7p15 deletion

Age (years), sex	Patient 1 Present case 13, male	Patient 2 Jun *et al.* (2011)[6] 4, male	Patient 3 Dunø *et al.* (2004)[5] case 1 5, female	Patient 4 Dunø *et al.* (2004)[5] case 2 4, male	Patient 5 Dunø *et al.* (2004)[5] case 3 21, male
Chromosomal deletion					
Location	7p15.3p15.1	7p15.3p15.1	7p15.3p14.3	7p15.2p14.2	7p15.3p14.2
Size (Mb)	6.9	5.6	9.8	9.0	12
Inheritance (parental origin)	De novo (paternal)	De novo	De novo	De novo	De novo (maternal)
Development					
Developmental delay	+	+	+	+	NA
Speech delay	+	+	+	+	NA
Limb anomaly					
Small hands and feet	+	+	+	+	NA
Clinodactyly of fingers	5th both	–	4th right	5th both	5th both
Other finger anomaly	–	Limited extension (1st, 2nd, 3rd)	Short fingers	Short fingers	Thumb anomaly
Great toe anomaly	Curved and broad	Hypoplasia	Short and broad	NA	Hypoplasia
Other toe anomaly	Short toes	NA	NA	Short toes pes planus	NA
Genital anomaly					
Genital abnormality	–	Hypospadias	NA	NA	Cryptorchidism
Facial features					
Low-set ears	+	+	NA	NA	+
Ear anomaly	Posterior rotated	Posterior angulated	NA	Short, slightly deformed	NA
Palpebral fissures anomaly	–	Upslanted	Upslanted	Downslanted	Upslanted
Flat nasal bridge	–	+	+	NA	NA
Nostril anomaly	–	NA	Anteverted	NA	Upturned
Forehead anomaly	Bifrontal narrowing	Frontal bossing	NA	NA	NA
Other facial anomaly	–	NA	Broad lips broad nose	Broad neck	Large mouth retrognathia
Other features					
Short stature	+	+	NA	+	NA
Neonatal feeding difficulty	+	+	NA	NA	+

+, feature present; –, feature absent; NA, not available.

no data on the relationship between *JAZF1* and neurodevelopment or brain function.[9]

Nonetheless, it remains inconclusive as to which genes are responsible for additional phenotypes in deletion+ HFGS. Further collection of cases of deletion+ HFGS will facilitate identification of responsible genes.

Acknowledgments

We are deeply grateful to the patient and his family for participating in this study. We also thank Professor Tadashi Ariga for his thoughtful advice on this report.

References

1 Goodman FR. Limb malformations and the human *HOX* genes. *Am. J. Med. Genet. A* 2002; **112**: 256–65.
2 Mortlock DP, Innis JW. Mutation of *HOXA13* in hand-foot-genital syndrome. *Nat. Genet.* 1997; **15**: 179–80.
3 Devriendt K, Jaeken J, Matthijs G *et al.* Haploinsufficiency of the *HOXA* gene cluster, in a patient with hand-foot-genital syndrome, velopharyngeal insufficiency, and persistent patent ductus botalli. *Am. J. Hum. Genet.* 1999; **65**: 249–51.
4 Hoover-Fong JE, Cai J, Cargiles CB *et al.* Facial dysgenesis: A novel facial syndrome with chromosome 7 deletion p15.1–21.1. *Am. J. Med. Genet. A* 2003; **117**: 47–56.
5 Dunø M, Hove H, Kirchhoff M, Devriendt K, Schwartz M. Mapping genomic deletion down to the base: A quantitative copy number scanning approach used to characterise and clone the breakpoints of a recurrent 7p14.2p15.3 deletion. *Hum. Genet.* 2004; **115**: 459–67.
6 Jun KR, Seo EJ, Lee JO, Yoo HW, Park IS, Yoon HK. Molecular cytogenetic and clinical characterization of a patient with a 5.6-Mb deletion in 7p15 including *HOXA* cluster. *Am. J. Med. Genet. A* 2011; **155A**: 642–7.
7 Hosoki K, Kagami M, Tanaka T *et al.* Maternal uniparental disomy 14 syndrome demonstrates Prader-Willi syndrome-like phenotype. *J. Pediatr.* 2009; **155**: 900–3.
8 Koontz JI, Soreng AL, Nucci M *et al.* Frequent fusion of the JAZF1 and JJAZ1 genes in endometrial stromal tumors. *Proc. Natl Acad. Sci. USA* 2001; **98**: 6348–53.
9 Zeggini E, Scott LJ, Saxena R *et al.* Meta-analysis of genome-wide association data and large-scale replication identifies additional susceptibility loci for type 2 diabetes. *Nat. Genet.* 2008; **40**: 638–45.

EUROPEAN JOURNAL OF PAEDIATRIC NEUROLOGY 15 (2011) 372–375

ELSEVIER

Official Journal of the European Paediatric Neurology Society

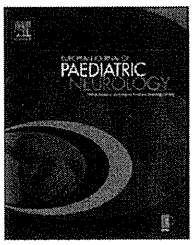

Case study

Iomazenil hyperfixation in single photon emission computed tomography study of malformations of cortical development during infancy

Norimichi Higurashi[a,b,*], *Shin-ichiro Hamano*[a], *Tomotaka Oritsu*[a,b], *Motoyuki Minamitani*[b,c], *Masayuki Sasaki*[d], *Hiroyuki Ida*[b]

[a] *Division of Neurology, Saitama Children's Medical Center, Japan*
[b] *Department of Pediatrics, Jikei University School of Medicine, Japan*
[c] *Division of Child Health and Human Development, Saitama Children's Medical Center, Japan*
[d] *Department of Child Neurology, National Center of Neurology and Psychiatry, Japan*

ARTICLE INFO

Article history:
Received 15 June 2010
Received in revised form
11 February 2011
Accepted 20 March 2011

Keywords:
Epileptogenesis
Gamma-aminobutyric acid
Hemimegalencephaly
Immaturity
Lissencephaly

ABSTRACT

We present 2 cases of malformations of cortical development and early onset epilepsy. The first case is of a patient with left hemimegalencephaly who developed focal epilepsy at the age of 2 days and cluster spasms at 1.5 months. After left functional hemispherectomy, seizures originated from the contralateral hemisphere, which had shown normal signals in the preoperative magnetic resonance imaging study. The second case is of a patient with lissencephaly, caused by a missense mutation in the doublecortin gene, who developed West syndrome at the age of 5 months. In both the cases, ^{123}I-iomazenil single photon emission computed tomography performed during infancy showed significant hyperfixation in the dysplastic lesions. This finding indicates the immaturity of the affected neurons and a gamma-aminobutyric acidergic involvement in epileptogenesis associated with malformations of cortical development during infancy.

1. Introduction

Malformation of cortical development (MCD) is one of the major causes of intractable childhood epilepsy.[1] Defects in some processes of corticogenesis, including migration, proliferation, or differentiation of neurons, can cause diverse types of MCDs. Here, we report 2 cases of patients with severe MCD and early onset epilepsy, who underwent ^{123}I-iomazenil single photon emission computed tomography (SPECT) during infancy. Neither of the patients had received benzodiazepines around the time of the SPECT scans.

2. Case study

2.1. *Case 1*

The patient was a boy with left hemimegalencephaly. His detailed clinical history, including seizure development

* *Corresponding author*. Department of Pediatrics, School of Medicine, Fukuoka University, 45-1, 7-chome, Nanakuma, Jonan-ku, Fukuoka 814-0180, Japan. Tel.: +81 92 801 1011; fax: +81 92 863 1970.
E-mail address: higijh.n@gmail.com (N. Higurashi).
1090-3798/$ – see front matter © 2011 European Paediatric Neurology Society. Published by Elsevier Ltd. All rights reserved.
doi:10.1016/j.ejpn.2011.03.007

associated with functional hemispherectomy, has been previously reported.[2] He experienced seizures consisting of motion arrest, apnoea, and facial cyanosis at the age of 2 days. Magnetic resonance imaging (MRI) revealed enlargement of and cortical dysplasia in the left cerebral hemisphere (Fig. 1A). The right hemisphere appeared to be normal, except for the slightly blurred grey-white matter demarcation in the medial orbito-frontal cortex and some frontocentral regions. Ictal electroencephalography (EEG) revealed that seizure activities originated in the left centro-parietal region. Valproate and phenobarbital were ineffective in ameliorating the seizures. At 1.5 months of age, the patient developed epileptic spasms in clusters. The EEG performed at the age of 2 months showed a suppression-burst pattern on the left side. Because of early onset intractable epilepsy, a left functional hemispherectomy was performed in another hospital, at the age of 3 months. However, intractable seizures originating from the right hemisphere developed shortly after the operation. Follow-up MRIs performed at the age of 7, 20, and 29 months showed frontocentral cortical lesions in the right hemisphere, with signs of progression of myelination, and an increase in the thickness of the cortex (Fig. 1D).

We performed ^{123}I-iomazenil SPECT twice before surgery. The first scan performed at age of 19 days showed significant hyperfixation in a large cortical area of the left hemisphere, particularly in the central region, and in the right frontocentral cortex (Fig. 1B), corresponding to the dysplastic lesions. Hyperfixation was also observed in the medial frontal and medial temporal regions. These findings were very distinct from the fixation patterns observed in the 3 control infants. All axial images of the control subjects are presented as Supplementary Figure, and some representative images of a 5-month-old boy with benign infantile convulsions are shown as Fig. 1H. The binding levels of iomazenil of the control subjects were high in the occipito-parietal region, especially in the primary visual cortex, and central region, but low in the fronto-temporal region. Although all the control infants suffered mild seizure episodes, they never had any other neurological abnormalities or organic lesions identifiable by MRI. The second SPECT performed at the age of 2 months showed reduced fixation in the frontal and the left parieto-temporal regions and enhanced fixation in the occipital cortex, which was considered a normal developmental change (Fig. 1C).

2.2. *Case 2*

The patient was a boy with type I lissencephaly caused by a missense mutation in doublecortin gene (c.2T > A). His postnatal psychomotor development was retarded. Cluster spasms appeared at the age of 5 months. His interictal EEG revealed a pattern of hypsarrhythmia, and hence, he was diagnosed with West syndrome. MRI performed upon admission revealed lissencephaly with an anterior severity in the anterior-posterior direction (Fig. 1E). The spasms were temporarily relieved by adrenocorticotropic hormone treatment. When he was 12-months-old, we added valproate to the treatment regimen. His seizures changed into focal seizures consisting of upward rolling of his eyeballs for a few seconds, and the seizure frequency decreased to a few times a day. The interictal EEG performed at the age of 17 months showed occasional spikes in the right occipital derivation.

^{123}I-iomazenil SPECT performed at the age of 6 months before the adrenocorticotropic hormone treatment, revealed pronounced hyperfixation across the entire cortex (Fig. 1F). This finding persisted in the follow-up scan at the age of 17

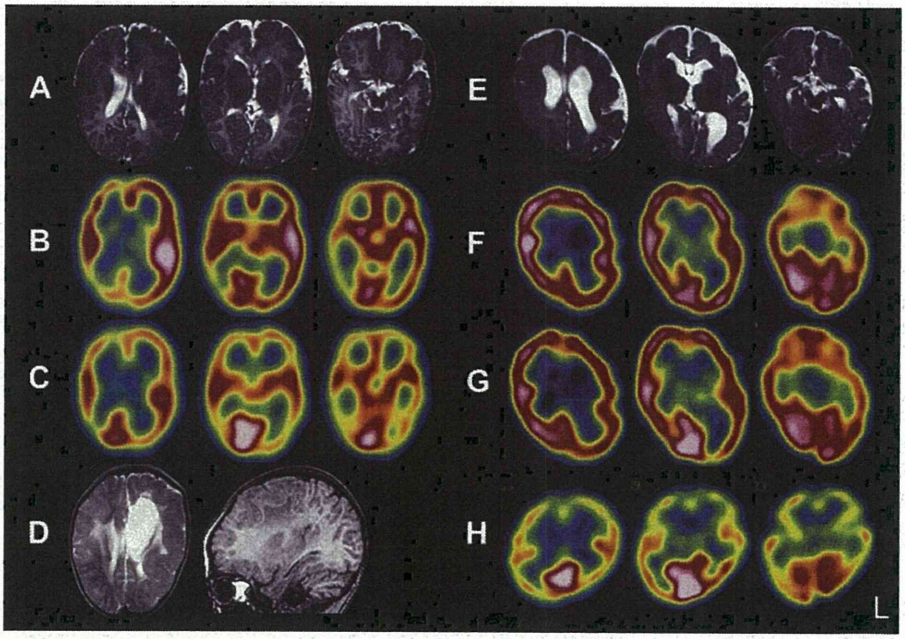

Fig. 1 – MRI and ^{123}I-iomazenil SPECT images of the 2 patients and a control subject. (A, E) T2-weighted images and (D) T2-weighted axial image (left) and T1-weighted sagittal image (right). (A–D) case 1: (A, C) 2 months, (B) 19 days, and (D) 29 months. (E–G) case 2: (E, F) 6 months, and (G) 17 months. (H) Control SPECT images of a 5-month-old infant with benign infantile convulsions. MRI, magnetic resonance imaging; SPECT, single photon emission computed tomography.

months (Fig. 1G). Compared to the control images (Supplementary Figure and Fig. 1H), the frontal hyperfixation was obviously abnormal; however, the hyperfixation in the occipital region, where the MRI showed a normal-shaped cortex, may be a physiological change.

3. Discussion

In both the patients with severe MCD, ^{123}I-iomazenil SPECT demonstrated abnormal hyperfixation in the lesions during early infancy. During normal development of the brain, postnatal neuronal maturation occurs early in the occipital and central regions and later in the frontal region. This development is corroborated by a synchronous progression of myelination and an increase in regional cerebral blood flow, which can be detected by MRI and SPECT. The images of the control infants in this study indicate that the iomazenil binding is symmetrically high initially in these regions, particularly in the occipital area, and is usually low in the fronto-temporal region during infancy (Supplementary Figure and Fig. 1H). In both patients, however, the hyperfixation areas extended beyond these physiological regions and included the frontal region. In case 1, the iomazenil binding in the left occipito-temporal region with a dysplastic cortex was asymmetrically higher than that in the right region with a normal-shaped cortex. Because ^{123}I-iomazenil SPECT is usually evaluated by visualizing the regional differences in the tracer binding level, we could not determine whether the absolute binding amount had increased in the dysplastic lesions. The relative fixation level, as compared to the physiological hyperfixation in the occipital region, however, indicates that the iomazenil binding in the lesions may have actually increased beyond the physiological level.

There are several potential mechanisms for the iomazenil hyperfixation in lesions. One of them is the association of abundant $GABA_A$ receptor expression with immaturity of the affected neurons and increased number of neurons and synapses. During brain development, GABA is the first active neurotransmitter, and it induces excitatory effects through $GABA_A$ receptors.[3] This GABAergic excitation has been found to be crucial to the progress in corticogenesis. A positron emission tomography study using flumazenil, a ligand of the $GABA_A$ receptor, suggested that $GABA_A$ receptor expression is higher in younger children.[4] These studies indicate that the immature neurons may express the abundant $GABA_A$ receptors.

In MCD lesions in paediatric patients, the presence of immature neurons and predominance of GABAergic synaptic activity have been demonstrated.[5] In addition, increased cortical thickness, delayed neurogenesis, and excessive neuro- and synaptogenesis have been suggested in hemimegalencephaly studies.[6,7] In case 1, the iomazenil hyperfixation in the cortical lesions might represent these actively ongoing abnormal corticogenesis. This notion is supported by the postnatal increase in the thickness of the dysplastic cortex in the right frontal lobe seen in this case. These results indicate that abundant expression of $GABA_A$ receptors in MCD lesions may play a critical role.

The excitatory GABAergic effects and abundant $GABA_A$ receptors in affected neurons may induce or enhance the epileptogenesis in MCDs during early infancy. Recent investigations indicate that the GABAergic excitation of immature neurons that are connected to the normal pyramidal cells might be crucial in inducing clinical seizures.[5,8,9] In the epileptogenic lesions of cortical dysplasia and hippocampal sclerosis, low expression of the potassium chloride co-transporter KCC2 has been identified.[10,11] The upregulation of KCC2 is crucial to the developmental and functional transition from excitatory to inhibitory GABAergic neurotransmission, which may start shortly after birth.[12] The failure of the upregulation of KCC2 would lead to prolonged excitation of the abundant $GABA_A$ receptors in the dysplastic lesions.

Another possible mechanism for iomazenil hyperfixation is the upregulation of postsynaptic $GABA_A$ receptors by a reduction in- or an impaired function of GABAergic neurons, as suggested in previous reports.[13,14] Interestingly, the involvement of *DCX* in the maturation of GABAergic neurons was recently reported.[8,15] The *DCX* mutation reported in case 2 supports this hypothesis.

In both the MCD cases reported, ^{123}I-iomazenil SPECT showed lesional hyperfixation during early infancy. This finding may be associated with the immaturity of the affected neurons and ongoing corticogenesis and may help in explaining epileptogenesis. Further investigation is required to elucidate the exact mechanisms and pathogenic significance of this finding.

Acknowledgement

We are deeply grateful to Dr. Mitsuhiro Kato, at the department of pediatrics, Yamagata University School of Medicine, for the genetic analysis of the doublecortin gene.

None of the authors has any conflict of interest to disclose.

Appendix. Supplementary material

The supplementary data associated with this article can be found in the on-line version at doi:10.1016/j.ejpn.2011.03.007.

REFERENCES

1. Verrotti A, Spalice A, Ursitti F, et al. New trends in neuronal migration disorders. *Eur J Paediatr Neurol* 2010;14:1–12.
2. Kometani H, Sugai K, Saito Y, et al. Postnatal evolution of cortical malformation in the "non-affected" hemisphere of hemimegalencephaly. *Brain Dev* 2010;32:412–6.
3. Wang DD, Kriegstein AR. Defining the role of GABA in cortical development. *J Physiol* 2009;587:1873–9.
4. Chugani DC, Muzik O, Juhasz C, et al. Postnatal maturation of human GABAA receptors measured with positron emission tomography. *Ann Neurol* 2001;49:618–26.
5. Cepeda C, Andre VM, Wu N, et al. Immature neurons and GABA networks may contribute to epileptogenesis in pediatric cortical dysplasia. *Epilepsia* 2007;48(Suppl. 5):79–85.
6. Mathern GW, Andres M, Salamon N, et al. A hypothesis regarding the pathogenesis and epileptogenesis of pediatric cortical dysplasia and hemimegalencephaly based on MRI

cerebral volumes and NeuN cortical cell densities. *Epilepsia* 2007;**48**(Suppl. 5):74–8.
7. O'Kusky JR, Akers MA, Vinters HV. Synaptogenesis in hemimegalencephaly: the numerical density of asymmetric and symmetric synapses in the cerebral cortex. *Acta Neuropathol* 1996;**92**:156–63.
8. Ackman JB, Aniksztejn L, Crepel V, et al. Abnormal network activity in a targeted genetic model of human double cortex. *J Neurosci* 2009;**29**:313–27.
9. Rheims S, Represa A, Ben-Ari Y, Zilberter Y. Layer-specific generation and propagation of seizures in slices of developing neocortex: role of excitatory GABAergic synapses. *J Neurophysiol* 2008;**100**:620–8.
10. Jansen LA, Peugh LD, Roden WH, Ojemann JG. Impaired maturation of cortical GABA(A) receptor expression in pediatric epilepsy. *Epilepsia* 2010;**51**:1456–67.
11. Huberfeld G, Wittner L, Clemenceau S, et al. Perturbed chloride homeostasis and GABAergic signaling in human temporal lobe epilepsy. *J Neurosci* 2007;**27**:9866–73.
12. Rivera C, Voipio J, Payne JA, et al. The K+/C1- co-transporter KCC2 renders GABA hyperpolarizing during neuronal maturation. *Nature* 1999;**397**:251–5.
13. Richardson MP, Koepp MJ, Brooks DJ, Fish DR, Duncan JS. Benzodiazepine receptors in focal epilepsy with cortical dysgenesis: an 11C-flumazenil PET study. *Ann Neurol* 1996;**40**: 188–98.
14. Jacobs KM, Kharazia VN, Prince DA. Mechanisms underlying epileptogenesis in cortical malformations. *Epilepsy Res* 1999; **36**:165–88.
15. Cai Y, Xiong K, Chu Y, et al. Doublecortin expression in adult cat and primate cerebral cortex relates to immature neurons that develop into GABAergic subgroups. *Exp Neurol* 2009;**216**:342–56.

ELSEVIER

Brain & Development 33 (2011) 379–383

BRAIN & DEVELOPMENT
Official Journal of the Japanese Society of Child Neurology

www.elsevier.com/locate/braindev

Original article

Effectiveness and safety of non-intravenous high-dose phenobarbital therapy for intractable epilepsy during childhood

Kenjiro Kikuchi [a,b,*], Shin-ichiro Hamano [a], Tomotaka Oritsu [a], Reiko Koichihara [a], Manabu Tanaka [a], Motoyuki Minamitani [a], Hiroyuki Ida [b]

[a] *Division of Neurology, Saitama Children's Medical Center, Japan*
[b] *Department of Pediatrics, Jikei University School of Medicine, Japan*

Received 12 February 2010; received in revised form 22 July 2010; accepted 23 July 2010

Abstract

High-dose phenobarbital (PB) therapy is effective for refractory status epilepticus. We reviewed medical records of patients with intractable partial epilepsies on whom performed non-intravenous high-dose PB therapy. Thirteen patients received PB rectally or orally at a dosage of 20–30 mg/kg/day initially, and the PB dosage was gradually reduced to a maintenance dosage of 5–10 mg/kg/day orally. We evaluated the effectiveness and safety of this procedure after 14 days at the maintenance dosage level. Twelve patients had partial seizures and one had secondary generalized seizures. In six of 13 patients (46%), seizure frequencies decreased more than 50%, and two of 13 patients (15%) became seizure free. In five of seven patients who were treated by continuous midazolam infusion therapy, we were able to discontinue the midazolam therapy. Adverse effects were found in seven of 13 patients. We were able to continue high-dose PB therapy in six patients because their adverse effects were transient and improved after a decrease in PB concentration, but we discontinued this therapy in the patient who developed Stevens–Johnson syndrome. Respiratory depression and hypotension were not found in our study. We conclude that high-dose PB therapy is effective and may be considered as an additional treatment for intractable partial epilepsy in childhood.

Keywords: High-dose phenobarbital therapy; Intractable partial epilepsy; Status epilepticus; Non-intravenous; Stevens–Johnson syndrome

1. Introduction

High-dose phenobarbital (PB) therapy, usually given intravenously, is effective for refractory status epilepticus [1,2]. In Japan, where intravenous PB therapy was not available until October 2008, there were some reports that non-intravenous high-dose PB therapy was effective for refractory status epilepticus [3–5]. In these reports, PB was given intramuscularly, rectally, or orally during high-dose PB therapy.

Only a few anecdotal studies reported that non-intravenous high-dose PB therapy was effective for intractable epilepsy in childhood as an additional therapy [6,7]. We performed non-intravenous high-dose PB therapy for intractable partial epilepsies during childhood, and evaluated the effectiveness and safety of this therapy.

2. Methods

We reviewed medical records of patients on whom non-intravenous high-dose PB therapy performed between January 1994 and July 2008 at Saitama Children's Medical Center, Saitama, Japan. Intractable partial epilepsy in this study was defined that epileptic partial seizures occurred daily even though we treated

* Corresponding author at: Division of Neurology, Saitama Children's Medical Center, 2100 Magome, Iwatsuki-ku, Saitama-city, Saitama 339-8551, Japan. Tel.: +81 48 758 1811; fax: +81 48 758 1818.
E-mail address: kikuchi.kenjiro@pref.saitama.lg.jp (K. Kikuchi).

0387-7604/$ - see front matter © 2010 The Japanese Society of Child Neurology. Published by Elsevier B.V. All rights reserved.
doi:10.1016/j.braindev.2010.07.009

Table 1
Patients' characteristics, outcome, and adverse effects in high-dose PB therapy.

Case	Sex	Age at high-dose PB therapy	Past history and/or complications	Seizure type (manifestations)	Concomitant AEDs	Duration of high-dose PB therapy (days)	PB serum levels at evaluation (μg/ml)	Seizure outcome	Adverse effect
1	F	2 mo	Neonatal asphyxia, mutlicystic encephalomalacia, West syndrome, MR	Tonic posturing of the legs, myoclonus of the arms	VPA	29	53	Effective	No
2	M	10 mo	MR	Rolling up of the eyes, apnea, clonic movements of the arms	CLB, ZNS, MDL infusion	21	69	Effective (seizure free)	Drowsiness
3	F	11 mo	Subcortical band heterotopia, MR	Head rotation to the right, tonic posturing of the arms	PHT, VPA	21	66	Effective (seizure free)	Drowsiness
4	M	4 yr 7 mo	MR	Rolling up of the eyes, tonic posturing of the arms	AZA, CZP, PRM, MDL infusion	24	38	Effective	No
5	F	5 yr 10 mo	Huntington disease, MR	Clonic movements of the arms	CBZ, VPA, MDL infusion	18	71	Effective	No
6	F	6 yr 9 mo	Acute encephalopathy, MR	Oral automatism, deviations of the eyes to the right	AZA, PB[b], PHT, MDL infusion	50	82	Effective	Emotional instability
7[a]	M	1 mo	Neonatal asphyxia, MR	Rolling up of the eyes, tonic posturing of the arms	MDL infusion	30	44	Not effective	No
8	M	3 mo	West syndrome, MR	Tonic posturing of the legs	MDL infusion	31	54	Not effective	No
9	M	5 mo	MR	Rolling up of the eyes, tonic posturing of the arms	PHT, VPA	41	27	Not effective	Drowsiness
10	F	8 mo	West syndrome, MR	Rolling up of the eyes	PHT	22	50	Not effective	Drowsiness
11	M	1 yr 7 mo Hypersecretion of saliva	West syndrome, MR	Clonic movements of the arms, oral automatism	CLB, VPA, ZNS	21	40	Not effective	
12	F	9 yr 7 mo	MR	Loss of consciousness,	CLB, ZNS, PB[b]	18	32	Not effective	No
13	M	11 yr 10 mo	MR	Tonic posturing of the arms, secondary generalization	CLB, PHT, TPM, VPA, MDL infusion	8	ND	Aborted	Stevens–Johnson syndrome, liver dysfunction

AEDs, antiepilptic drugs; AZA, acetazolamide; CBZ, carbamazepine; CLB, clobazam; CZP, clonazepam; F, female; M, male; MDL, midazolam; MR, mental retardation; MRI, magnetic resonance imaging; ND, not done; mo, month; PB, phenobarbital; PHT, phyntoin; PRM, primidone; TPM, topiramate; VPA, valpric acid; yr, year; ZNS, zonisamide.

[a] All cases, except Case 7, were received rectal high-dose PB therapy initially. Only Case 7 was received oral high-dose PB therapy initially.

[b] PB was administered orally at standard dose.

by oral antiepileptic drugs (AEDs) or continuous intravenous midazolam (MDL) therapy. All patients were hospitalized in our institution, and were treated. Medical records were reviewed as follows: age at high-dose PB therapy, past history and/or complications, seizure type, concomitant AEDs when high-dose PB therapy performed, dosage of PB, PB serum level, the duration of high-dose PB therapy, seizure outcome, interictal electroencephalogram (EEG) findings, and adverse effects.

Patients received PB orally or rectally at a dosage of 20–30 mg/kg/day initially for 2–4 days, after which the PB dosage was gradually reduced to the maintenance dosage of 5–10 mg/kg/day, as previous studies examined [6,7]. After that, all of the patients received oral PB medications at the same maintenance dosage. No AEDs were added during high-dose PB therapy.

We evaluated the effectiveness and safety of high-dose PB therapy after 14 days at the oral maintenance dosage level, because the duration of the PB serum level at steady-state was about 14 days. We evaluated the effectiveness of this therapy as follows: "Effective" represented a greater than 50% seizure reduction, "Not effective" represented a less than 50% seizure reduction, and "Exacerbation" represented an increase in seizure frequency.

3. Results

High-dose PB therapy was performed on 13 patients (seven males and six females). The age range of the patients who received high-dose PB therapy was 1 month to 11 years, and the age range of the patients at the onset of epilepsy was 1 month to seven years (Table 1). Only one patient (Case 7 in Table 1) was received oral high-dose PB therapy from the beginning of this therapy. A history of neurological disorders was found in all 13 patients: mental retardation in 13 patients, West syndrome in four, neonatal asphyxia in two, Huntington Disease in one, and acute encephalopathy in one. The four patients who previously had West syndrome underwent a combination therapy of vitamin B6, γ-globulin, adrenocorticotropic hormone (ACTH) therapy, and thyrotropin-releasing hormone (TRH) therapy. Abnormal findings of magnetic resonance imaging (MRI) were found in nine patients (69%): cerebral atrophy in six patients, multicystic leukoencephalomalacia in one, subcortical band heterotopia in one, and cerebellar atrophy in one. Partial seizures were found in 12 patients and secondary generalized seizures in one, but primary generalized seizures were not found. Seizures with motor component, such as tonic posturing and clonic movements, were common in 10 of 13 patients.

The concomitant AEDs were shown in Table 1 when non-intravenous high-dose PB therapy had performed. Phenytoin and valproic acid was used for five patients, clobazam for four, zonisamide for three, acetazolamide and PB for two, and carbamazepine, clonazepam, primidone, and topiramate for one. MDL continuous infusion therapy was performed on seven patients, who had no complications induced by changes in medication, intercurrent infections, acute neurological insults such as meningitis, trauma, and anoxia. Four of seven patients who received MDL therapy had status epilepticus (Cases 5, 6, 8, and 13 in Table 1). Other three patients had repetitive partial seizures more than 20 times per day (Cases 2, 4 and 7).

In six of the 13 patients (46%), non-intravenous high-dose PB therapy was effective, and two of them (Cases 2 and 3) became seizure free. We were able to discontinue MDL continuous infusion in five patients (71%). Concerning seizure type, this therapy was effective in five of nine patients who had seizures with motor components such as tonic posturing and clonic movements. There was no difference in the duration (average ± standard deviation days) of non-intravenous high-dose PB therapy between the patients for whom this therapy was effective and not effective, 27.2 ± 11.8 and 27.2 ± 8.5 days, respectively. The average PB serum level at evaluation was 63.2 μg/ml among the patients for whom high-dose PB therapy was effective, and 41.1 μg/ml among the patients for whom high-dose PB therapy was not effective. Concerning interictal EEG findings, all patients had frequently multifocal and/or generalized electric abnormalities, such as spikes, polyspikes, spike-wave complexes, and high-amplitude high voltage slow waves. In the patients for whom this therapy was effective, the frequencies of these abnormalities decreased and generalization disappeared, whereas there were no changes of electric abnormalities in the patients for whom this therapy was not effective.

Adverse effects during the high-dose PB therapy were found in seven patients (54%): drowsiness in four patients, emotional instability in one, hypersecretion of saliva in one, and Stevens–Johnson syndrome in one. Drowsiness and emotional instability disappeared as the PB serum level decreased. Case 11 in Table 1 needed mandatory respirator support because hypersecretion of saliva obstructed his airway. Case 13 in Table 1 presented with Stevens–Johnson syndrome and liver dysfunction; we therefore discontinued high-dose PB therapy. He recovered after steroid therapy without any sequelae. In our study, respiratory depression and hypotension were not found.

4. Discussion

The present study showed that non-intravenous high-dose PB therapy was effective for intractable partial epilepsy in childhood. A reduction of more than 50% of seizure frequency was found in 46% of the patients, and discontinuation of MDL continuous infusion was in 71%. Adverse effects were found in seven patients; those in six patients were transient and improved after